

## SPATIOTEMPORAL DYNAMICS OF SINGLE-LETTER READING: A COMBINED ERP-FMRI STUDY

S. CASAROTTO<sup>1,2,7\*</sup>, A.M. BIANCHI<sup>2</sup>, E. RICCIARDI<sup>1,3,6</sup>, C. GENTILI<sup>4,6</sup>,  
N. VANELLO<sup>5,6</sup>, M. GUAZZELLI<sup>4</sup>, P. PIETRINI<sup>1,3</sup>, G.A. CHIARENZA<sup>7</sup>,  
S. CERUTTI<sup>2</sup>

<sup>1</sup> Laboratory of Clinical Biochemistry and Molecular Biology, Department of Experimental Pathology, Medical Biotechnologies, Infectivology, and Epidemiology, University of Pisa, Pisa, Italy; <sup>2</sup> Department of Biomedical Engineering, IIT Unit, Polytechnic University of Milan, Milan, Italy; <sup>3</sup> Department of Laboratory Medicine and Molecular Diagnostics, AUO Pisa, Italy; <sup>4</sup> Unit of Clinical Psychology, AUO Pisa, Department of Psychiatry, Neurobiology, Pharmacology, and Biotechnologies, University of Pisa, Pisa, Italy; <sup>5</sup> Department of Information Engineering, University of Pisa, Pisa, Italy; <sup>6</sup> Magnetic Resonance Imaging Laboratory, Fondazione "G. Monasterio", CNR/Regione Toscana, Pisa, Italy; <sup>7</sup> Department of Child and Adolescent Neuropsychiatry, AO "G. Salvini", Rho Hospital, Rho, Milan, Italy

### ABSTRACT

This work investigates the neural correlates of single-letter reading by combining event-related potentials (ERPs) and functional magnetic resonance imaging (fMRI), thus exploiting their complementary spatiotemporal resolutions. Three externally-paced reading tasks were administered with an event-related design: passive observation of letters and symbols and active reading aloud of letters. ERP and fMRI data were separately recorded from 8 healthy adults during the same experimental conditions. Due to the presence of artifacts in the EEG signals, two subjects were discarded from further analysis. Independent Component Analysis was applied to ERPs, after dimensionality reduction by Principal Component Analysis: some independent components were clearly related to specific reading functions and the associated current density distributions in the brain were estimated with Low Resolution Electromagnetic Tomography Analysis method (LORETA). The impulse hemodynamic response function was modeled as a linear combination of linear B-spline functions and fMRI statistical analysis was performed by multiple linear regression. fMRI and LORETA maps were superimposed in order to identify the overlapping activations and the activated regions specifically revealed by each modality. The results showed the existence of neuronal networks functionally specific for letter processing and for explicit verbal-motor articulation, including the temporo-parietal and frontal regions. Overlap between fMRI and LORETA results was observed in the inferior temporal-middle occipital gyrus, suggesting that this area has a crucial and multifunctional role for linguistic and reading processes, likely because its spatial location and strong interconnection with the main visual and auditory sensory systems may have favored its specialization in grapheme-phoneme matching.

---

\* Corresponding Author: Silvia Casarotto, Laboratory of Clinical Biochemistry and Molecular Biology, University of Pisa, Via S. Zeno, 61, 56127 Pisa (Italy). Tel.: +39 050 2213323. Fax: +39 050 2213322. E-mail: silvia.casarotto@bioclinica.unipi.it

## INTRODUCTION

Cognitive processes in humans are subserved by functionally specialized neuronal networks that can be investigated in the temporal and spatial domain, thanks both to the development of new technologies for functional exploration, and to the improvement of image and signal processing (5). Brain functional activity can be measured *directly*, by recording the electric/magnetic field generated by cortical neurons from the scalp (electro-/magneto-encephalography, EEG/MEG), or *indirectly*, by mapping the metabolic changes of cortical and sub-cortical nuclei (functional magnetic resonance, fMRI) (9). The EEG, a real-time blurred summation of local field potentials, has excellent time but unsatisfactory spatial resolution, since the problem of finding source configuration from scalp recordings (*inverse problem*) is undetermined (4). fMRI measures local changes in oxygen consumption resulting from neuronal metabolic activity, and has superior localization capabilities but low temporal resolution, due to the low-pass filtering characteristics of the hemodynamic response (58).

The possibility to combine the temporal and spatial properties of EEG and fMRI may in fact be useful to investigate brain functions from different perspectives, and to overcome the limitations related to individually applied modalities by exploiting their complementary spatiotemporal resolutions (70, 22, 95, 42, 1, 2, 3, 37, 59, 39, 71, 7). However, several methodological issues related to simultaneous recording of the two signals remain still unsolved (57, 32, 30, 45). Separate acquisitions of EEG and fMRI data may be accepted when the functional event/brain state of interest is reliably repeatable in different, but close in time, sessions, or when the same experimental paradigm is exactly reproduced in both sessions. In these conditions, the artifacts related to mutual interference between EEG and fMRI equipments are fully abolished (11, 63, 94).

Reading aloud implies a cerebral process perfectly suitable for investigation with different methodologies (25). Actually, reading aloud always activates a complex neuronal circuitry, involving the primary occipital visual cortex for perceiving written characters, the temporal auditory cortex for grapheme-phoneme matching, the motor and premotor cortex for articulation, and the associative cortex for evaluation of auditory feedback and comprehension (86, 38, 49, 74). Functional studies have confirmed that the left middle-superior temporal gyrus (Brodmann's area: BA 39), inferior parietal cortex (BA 40), precuneus (BA 7) and inferior frontal gyrus (BA 6/44), the bilateral fusiform gyrus (BA 19/37) and supplementary motor area (BA 6) are implied in reading (68, 29, 74, 83, 50). From a temporal perspective, EEG/MEG studies have demonstrated that the visual characteristics of letters/words are analyzed between 50 and 100 ms after stimulus presentation, thus generating early perceptive potentials (97, 90, 61). The conversion from visual to linguistic analysis likely occurs between 150 and 230 ms (97, 90, 61). The brain regions responsible for higher order cognitive functions, such as semantic analysis, feedback processes and memory are supposed to be later recruited.

This work proposes to investigate the spatiotemporal brain dynamics of single-letter reading by combining event-related potentials (ERPs) and fMRI data, separately recorded during the same experimental conditions, already validated by our group with ERP recordings in children (14, 16). Learning the correspondence between letters and speech

sounds is a basic aspect of reading acquisition, thus single letters represent a more suitable stimulus than letter strings for studying early reading processes (50). However, the use of single letters is quite infrequent in the literature, while letter strings and words are often preferred. Single-letter reading is a multistep process with a characteristic temporal evolution and is accomplished by the activation of a broad sensory-motor-cognitive neuronal network. Furthermore, brain response to visual presentation of single letters is able to predict reading success and to distinguish adult dyslexics better than words (28, 83). In the present experiment, grapheme-phoneme association is explicitly investigated through overt reading of the letters. Differently from a previous ERP-fMRI study of word reading by Vitacco et al. (105), an event-related design is applied to acquire artifact-free signals, to facilitate inter-modality integration, and to reduce the problem of speech-related movements.

## METHODS

### *Subjects*

Eight healthy right-handed adults (four male, four female; age range 22-36 years, native Italian speakers) were enrolled in the experiment. All participants underwent clinical, neurological and psychiatric examinations and laboratory tests (including routine blood and urine tests, liver, renal and endocrinological panels, EEG, structural brain MRI) to rule out history or presence of abnormal psycho-motor and language development, and of any relevant medical, neurological or psychiatric disorders and use of substance that could affect brain function or metabolism. All subjects were non-smokers, and had been medication-free for at least 4 weeks prior to the study, including over-the-counter medications. Written informed consent approved by the Local Ethical Committee was obtained from all participants prior to their enrolment into the study and after explanation of the study procedure and of the risks involved.

### *Experimental paradigm*

ERP and fMRI data were acquired during separate sessions with the same experimental protocol already validated by our group with ERP recordings in children (14, 16). A rapid event-related (ER) design with jittered inter-stimulus interval (ISI) and randomized stimulus delivery was applied (Fig. 1). Stimulation was provided and regulated using Presentation® (Version 0.76, <http://www.neurobs.com>). White single characters (Latin capital and small letters and non-alphabetic symbols) were visually presented for 20 ms on a black background. The angle of reading was about 1° in the ERP session and 2° in the fMRI session. Inter-stimulus interval (ISI) was always an integer multiple of 500 ms and was randomly chosen from a decreasing exponential distribution with maximum value at ISI minimum. In order to avoid temporal overlapping between successive event-related neural potentials, minimum ISI was set to 4 s in the ERP session. The hemodynamic responses to successive events are temporally overlapping unless ISI is longer than 10-15 s. However, long ISI likely reduces the attention level of participants, especially when tasks are simple, and induces a brain response not comparable with the ERP session. Therefore, minimum ISI was fixed at 2 s, and stimulus ordering was randomized so that the overlapping hemodynamic responses could be disentangled with the least amount of unexplained variance. Two conditions were applied: *passive* condition consisted in simply watching at randomly ordered letters and symbols, that were sorted *a posteriori* for estimating stimulus-specific responses; *active* condition consisted in reading aloud (i.e. *naming*) randomly ordered letters. Then, the following three tasks were obtained: *letter presentation*, *symbol presentation*, and *letter recognition* (i.e. *naming*). Data acquisition was partitioned into periods of continuous recording, labeled runs, each lasting about 4 min and containing 50 stimuli (25 letters and 25 symbols for passive condition and 50 letters for active condition). We estimated that 6 passive and 3 active runs per subject provided enough data for satisfactory signal-

## Event-related experimental paradigm

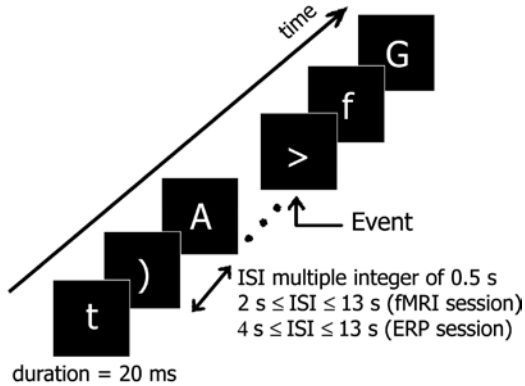


Fig. 1. – Event-related experimental paradigm: an “event” consisted in the visual presentation of a white-colored stimulus on a black background for 20 ms; stimuli were randomly ordered letters and symbols during passive condition and randomly ordered letters during active condition (see text for details); inter-stimulus interval (ISI) was randomly chosen as a multiple integer of 0.5 s; minimum ISI was 2 s in the fMRI session and 4 s in the ERP session.

Systems, Milwaukee, WI) with a standard birdcage head coil at the Magnetic Resonance Imaging Laboratory, Fondazione “G. Monasterio”, CNR/Regione Toscana, Pisa, Italy. At the beginning of the scanning session, a high resolution structural scan was acquired in the sagittal plane using a 3D GRASS sequence with TE = 5.22 ms, Repetition Time (TR) = 12.1 ms, FOV = 240 mm with 256 x 256 acquisition matrix (0.94 x 0.94 mm in-plane resolution) and 120 slices (1.2 mm thickness). Afterwards, multi-slice echo-planar images (EPIs) were axially acquired with TE = 40 ms, TR = 2 s, FOV = 240 mm with 64 x 64 acquisition matrix (3.75 mm x 3.75 mm in-plane resolution) and 22 contiguous 5-mm slices. Each functional run consisted of 115 brain volumes. Head movements were limited by carefully placed constraints. Stimuli were projected onto a screen located near the bottom of the bore and viewed from a mirror mounted on the head coil.

### Data analysis

**ERPs pre-processing.** Single-trial ERPs were pre-processed as described in Casarotto et al. (14) for reducing ocular artifacts and then visually inspected for rejecting residually artifact-contaminated trials. For each subject and task, averaged ERPs were computed from a minimum of 40 trials. Due to the presence of numerous artifacts in the EEG signals, two (male) out of eight subjects were discarded from further analysis.

**Spatial component analysis of ERPs.** Independent Component Analysis (ICA) separates a set of signals into their independent constituents components (ICs). ICA was applied to multi-channel averaged ERPs, assuming that the independent components represent the contribution of distinct neural sources that mix their activities into scalp recordings. We applied “infomax” ICA method (6) as implemented in the *runica* algorithm of the EEGLAB toolbox (24) (<http://scn.ucsd.edu/eeglab>). *Runica* estimates temporally independent and spatially fixed components by minimizing the mutual information between signals; under certain conditions, this computation is equivalent to maximizing joint entropy.

to-noise ratio (SNR) of averaged ERPs and statistical power of fMRI signal. The order of runs was randomized across subjects, but was not altered between the ERP and fMRI sessions.

### Data recording

**ERPs.** Electrophysiological data were recorded at the Neuro-physio-pathology Laboratory, Department of Child and Adolescent Neuropsychiatry, Azienda Ospedaliera “G. Salvini”, Rho Hospital, Rho, Milan, Italy. EEG was recorded from 19 electrodes referred to linked earlobe (33), integrated in an elastic cap, and placed according to the standard 10-20 system (Brainquick 2400, Micromed@, Italy). EOG was bipolarly recorded using 2 electrodes placed over and below the right eye. EEG and EOG recordings were band-pass filtered between 0.02-30 Hz and sampled at 256 Hz, with 4 s analysis time, 2 s pre- and 2 s post-stimulus. During the test, subjects were sitting in a dimly illuminated, electrically and acoustically shielded room and stimuli were displayed on a CRT screen.

**fMRI.** Imaging was performed on a 1.5T MRI scanner (GE Signa; GE Medical

Averaged ERPs, stored in matrix  $\mathbf{X}$ , were modeled as a linear combination of unknown sources organized in matrix  $\mathbf{S}$  (eq. 1):

$$\underset{m,T}{\mathbf{X}} = \underset{m,n}{\mathbf{A}} \cdot \underset{n,T}{\mathbf{S}} \quad (1)$$

with  $T$  = number of time samples in each trace,  $m$  = number of scalp sensors and  $n$  = number of sources. Matrix  $\mathbf{A}$  defines the relationship between neural sources and scalp measurements in terms of spatiotemporal superimposition and is therefore labeled *mixing matrix*. ICA recovers the original sources  $\mathbf{S}$  from just the observations  $\mathbf{X}$  through the estimation of an *unmixing matrix*  $\Psi$  (eq. 2):

$$\hat{\mathbf{S}} = \Psi \cdot \mathbf{X} \quad (2)$$

The  $j$ -th row of  $\hat{\mathbf{S}}$  represents the time course of relative strength or activity level of the  $j$ -th *component activation* or *independent component (IC)*. The element  $(i,j)$  of matrix  $\mathbf{A}$  gives the relative projection strength of the  $j$ -th IC into the  $i$ -th scalp sensor. The contribution of the  $j$ -th IC into the original data channels is computed as the product of the  $j$ -th column of  $\mathbf{A}$  with the  $j$ -th row of  $\mathbf{S}$  and is in original units (e.g.  $\mu\text{V}$ ). The assumption of linear and instantaneous mixing is perfectly legitimate for ERP data, because scalp recordings sum up the activity of attenuated sources without transmission delays (76). The following further assumptions hold: i) *measurements are noiseless or noise is negligible*: this hypothesis seems unrealistic but still allows to separate sources of interest even if these remain contaminated by measurement noise; ii)  *$\mathbf{A}$  is stationary*: this assumption is fully verified in the case of brain signals because the mixing of sources as measured by sensors does not change with time; iii) *the components are temporally independent of one another*.

In order to simplify computations, we assumed  $m = n$ , i.e. a square mixing matrix. However, the number of sources can be assumed to be smaller than the EEG sensors: therefore, Principal Component Analysis (PCA) was applied to reduce data dimensionality before ICA. Mathematically, PCA models a set of  $m$  signals as a linear combination of  $m$  principal components (PCs), that are orthogonal and account for the maximal amount of spatial variance of original data in the least square sense (27, 53, 52). ICA was applied after ERPs were reconstructed from the first  $k$  PCs altogether representing more than 95% of the data variance. This subtraction did not alter ERPs morphology and allowed to obtain only  $k$  ICs for further analysis.

*Neural source estimation.* The problem of estimating neural sources from scalp-recorded ERPs was solved by Low Resolution Electromagnetic Tomography method (LORETA<sup>®</sup> – <http://www.unizh.ch/keyinst/NewLORETA/LORETA01.htm>) (81): this approach directly computes the current density distribution in the brain, modeled as a three-compartment spherical head model registered to a standardized stereotactic space (96) available as a digitized MRI from the Brain Imaging Centre (Montreal Neurological Institute, MNI305). Solution space was restricted to cortical grey matter according to the digitized Probability Atlases also available from the Brain Imaging Centre (Montreal Neurological Institute): a voxel was labelled as grey matter if its probability of being grey matter (a) exceeded 33%, (b) exceeded the probability of being white matter, and (c) exceeded the probability of being cerebrospinal fluid. Brain volume was represented as a discrete 3D dense cubic grid with elementary sources located on grid points. Grid spacing was 7 mm and the total number of voxels was 2394. LORETA solution to the *inverse problem* is the smoothest 3D linear one among the infinite source configurations that generate the same scalp potentials. Therefore, the spatial resolution of LORETA maps is typically low, i.e. the estimated current distribution is a “blurred-localized” image of a point source: the location of maximal activity is preserved with a certain degree of dispersion. Physiologically, this approach may be explained by observing that neighboring neurons are generally simultaneously and synchronously active: therefore, neighboring grid points are more likely to be synchronized (i.e. of similar orientation and strength) than far grid points. EEG electrode coordinates were achieved using cross-registrations between spherical and realistic head geometry (99) (see Appendix A).

LORETA maps were estimated from each independent component, normalized and then averaged across subjects. Normalization consisted in linearly scaling the LORETA current density

values between 0 and 1, followed by transformation to  $z$ -score (mean subtraction and division by standard deviation) and thresholding at  $z = 1.96$  ( $p < 0.05$ ). Since the distribution of current density values in the brain may have very different dynamic ranges across subjects and tasks, this operation allowed to make the LORETA maps more comparable and to define a univocally recognizable threshold (100).

*fMRI analysis.* Structural and functional images were analyzed with the AFNI (Analysis of Functional NeuroImages) software (<http://afni.nimh.nih.gov/afni/>) (20). The following pre-processing steps were applied to fMRI data before statistical analysis: i) slice timing correction to align all slices to the same time origin; ii) rigid head movements correction with an heptic polynomial interpolation to register all brain volumes to the scan closest to acquisition of anatomical images using; iii) spatial smoothing with a 5 mm-FWHM Gaussian filter to reduce noise and increase functional overlap between runs and subjects; iv) normalization of image values to global mean intensity to calculate the percent signal change; v) concatenation of runs and masking of non-brain regions.

The BOLD (Blood Oxygenation Level Dependent) time series at each voxel was described by a multiple linear regression model and least squares method was used to estimate model coefficients. Stimulus timing was represented as a succession of unit impulse functions (Kronecker delta), that were convolved with the impulse hemodynamic response function (HRF). In order to better fit raw data, i.e. to account for physiological regional and inter-subject variability, a variable-shape BOLD response model was preferred to a fixed-shape one. Trial averaging could not be applied because successive stimuli were presented too close in time. Classical deconvolution methods are based on the estimation of the amplitude of TR-locked (i.e. synchronous and in-phase with the TR period) samples, thus allowing for arbitrary HRF shapes: in the present study, since TR is 2 s and ISI is an integer multiple of 0.5 s, four samples per TR would be necessary to correctly model all stimuli occurrence. Unfortunately statistical power rapidly decreases with the number of parameters to be estimated. Therefore, it was necessary to develop a variable-shape HRF with a limited number of parameters and perfectly defined at any arbitrary point in time. A linear combination of three linear B-spline basis functions, peaking at 0 s, 4 s, and 8 s after visual stimulus presentation (eq. 3, Fig. 2) (89) perfectly satisfied these constraints, and was used to model the impulse HRF to each task separately:

$$\begin{aligned}
 s_j(t) = & \sum_{k=1}^K \left[ \beta_{j,1}^k \cdot \text{tent}\left(\frac{t}{4}\right) + \beta_{j,2}^k \cdot \text{tent}\left(t - \frac{4}{4}\right) + \beta_{j,3}^k \cdot \text{tent}\left(t - \frac{8}{4}\right) \right] + \dots \\
 & \dots \sum_{h=1}^9 \left[ a_{j,h} + b_{j,h} \cdot t + c_{j,h} \cdot t^2 \right] + \dots \\
 & \dots \sum_{i=1}^6 m_{j,i} M_i(t) + n_j(t)
 \end{aligned} \tag{3}$$

where  $j$  is voxel index;  $K$  is the total number of tasks;  $h$  is the run index;  $\text{tent}(\frac{t-\tau}{b})$  is a linear B-spline function peaking at  $t = \tau$  s after stimulus presentation and lasting  $2b$  s;  $M_i(t)$  are the estimated rigid head motion parameters (3 for translation and 3 for rotation around the main axes);  $n(t)$  is noise term; a quadratic polynomial ( $a_j + b_j t + c_j t^2$ ) accounted for baseline. Model fitting to raw data produced an estimate of the model coefficients  $\beta_{j,1}$ ,  $\beta_{j,2}$ ,  $\beta_{j,3}$ ,  $a_{j,h}$ ,  $b_{j,h}$ ,  $c_{j,h}$ , and  $m_{j,i}$  at each voxel.

General linear tests (GLTs) [program 3dDeconvolve in AFNI software] (107) were performed for each subject and task separately with the null hypothesis  $\beta_1 + \beta_2 + \beta_3 = 0$ , i.e. searching in which brain regions the sum of the three model coefficients of interest is significantly different from zero. Single-subject image statistics were warped into a common standard space (96) and spatially resampled with linear interpolation to cubic 1 mm voxels before group analysis. Group maps of each task were estimated by one-sample t-test analysis, with  $p < 0.01$  and minimum cluster

size 577  $\mu\text{l}$ , corresponding to an overall significance of 0.048 according to Monte Carlo simulations [program AlphaSim in AFNI software] (106).

## RESULTS

*Spatial component analysis of ERPs.* Systematic inspection of the spatial distribution and time course of single independent components extracted from averaged ERPs (Fig. 3) identified distinctive patterns that resulted similar across subjects, and well resembled the reading potentials described in previous studies (16, 35, 56, 65).

Specifically, Chiarenza and colleagues (16) described the time course of the cerebral potentials before, during, and after self-paced letter recognition (i.e. *naming*) by superimposing the electromyographic (EMG) activity of the forearm flexor muscles, activated by button pressing, and of the lips, activated by overt articulation. Potentials were subdivided into four main periods (Fig. 4, adapted from ref. 15): *preparatory* (before EMG arm onset) including the Bereitschaftspotential (BP) associated to preparation of movement (54, 18); *pre-lexical* (between EMG arm onset and EMG lips onset, i.e. -200 – 150 ms), including Motor Cortex Potential (MCP) (80, 17), P0, N1, P1 waves related to attention and perceptual processes; *lexical* (between EMG lips onset and peak, i.e. 150 – 500 ms), including N2, P2a, P2b, N3, P4, N4 waves concerned with phonological analysis and stimulus feedback; and *post-lexical* (following EMG lips peak, i.e. > 500 ms), including P600 and LNA (Late Negative Area) potentials dealing with long-term memory and categorization mechanisms.

In the current study, one IC could be associated to the potentials N2 and P2b, i.e. a negativity occurring at about 180 ms and a positivity occurring at about 300 ms, in all tasks both predominant on the posterior regions. Another IC resembled the potential P2a, i.e. a positivity occurring at about 200 ms with fronto-central distribution. Only during tasks presenting Latin letters, an additional IC was reliably related to LNA, i.e. a wide slow negativity occurring between 0.5 – 1 s: during letter presentation task this component was more prominent in the fronto-central areas and was defined as LNAf, while during letter recognition task it was more posteriorly distributed and defined as LNAo.

*Distributed source imaging.* Table I and Fig. 5 show brain regions significantly activated during the three different reading tasks. LORETA maps were characterized by suprathreshold regions in both hemispheres, mainly in the lateral temporal and parietal lobes.

Neural sources of N2\_P2b component common to all tasks were distributed in the supramar-

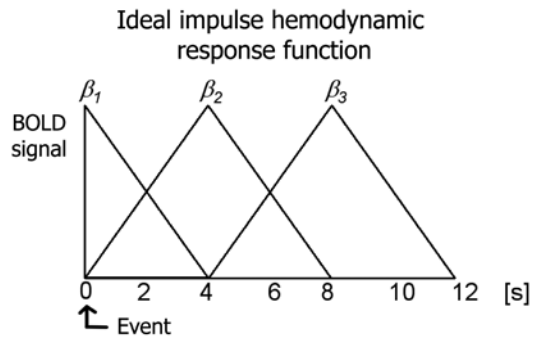


Fig. 2. – Ideal impulse hemodynamic response function was modeled as a linear combination of three linear B-spline basis functions peaking at 0, 4, and 8 s after event occurrence and with 4 s half-duration. Multiple linear regression analysis provided the estimation of the peak amplitude of the three basis functions ( $\beta_1$ ,  $\beta_2$ ,  $\beta_3$ ) for the *letter presentation*, *symbol presentation* and *letter recognition* (i.e. *naming*) tasks.

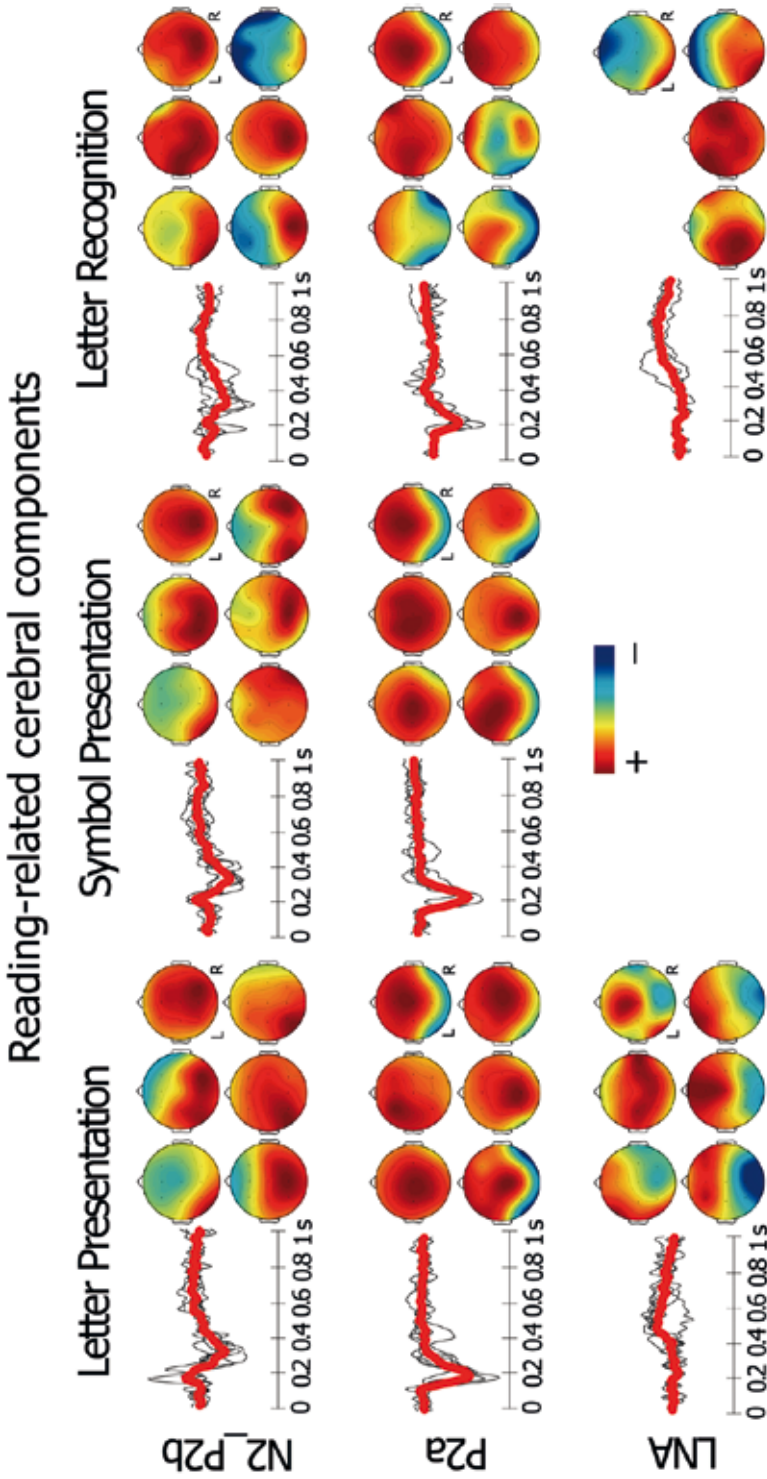


Fig. 3. – Time course and scalp map of the N2\_P2b, P2a, and LNA independent components extracted from averaged ERPs during *letter presentation*, *symbol presentation* and *letter recognition* tasks. Mean time course averaged across 6 subjects for each component and task (red line) is superimposed to individual time courses (black lines) within the temporal window 0 – 1 s after stimulus presentation. Spatial distribution of the components for each subject is reported with color-coded scalp maps from red (positive coefficient) to blue (negative coefficient). R = right; L = left.

ginal gyrus (BA 40), temporal lobe (BA 20/21/22/41/42), and angular gyrus (BA 19/22/37/39). These sources were essentially left-lateralized, especially during letter recognition that did not show any significant right lateral activation. Additional sources were present bilaterally in the cingulate (BA 23/30/31), occipitotemporal gyrus (BA 17/18), and middle precuneus (BA 7/31). During letter presentation and recognition only, N2\_P2b sources were observed in the left inferior temporal–middle occipital gyrus (BA 19/37), i.e. the fusiform gyrus.

The P2a component was generated by bilateral sources in the lateral temporal cortex (BA 20/21/22/41/42), angular gyrus (BA 19/22/37/39), and fusiform gyrus (BA 19/37), similarly in all tasks. However, while during letter presentation and recognition the activation was nearly bilateral and symmetrical, slightly weaker on the right, during symbol presentation the involvement of the right hemisphere was limited to the angular gyrus and superior temporal gyrus.

Furthermore, during symbol presentation additional activations were present in the medial cingulate (BA 23/30/31) and middle precuneus (BA 7/31). Similarly to N2\_P2b, P2a component was related to a left-lateralized source in the supramarginal gyrus in all tasks.

The late component LNAf identified during letter presentation mainly involved the medial cingulate (BA 23/30/31) and precuneus (BA 5/7/31). Conversely, the neural sources of LNAo component present during letter recognition were predominantly located in the left supramarginal gyrus (BA 40), superior temporal gyrus (BA 41/42), angular gyrus (BA 19/22/37/39), and fusiform gyrus (BA 19/20/37). Additional sources were observed in the medial inferior frontal gyrus (BA 10/11) and anterior cingulate (BA 24/32).

*Functional activation maps.* A prevalent involvement of the left as compared to the right hemisphere was found across all tasks (Table I, Fig. 5). Only letter recognition elicited a significant activation of right brain areas, specifically in the frontal cortex (BA 6/9/44), insula (BA 13), and middle-inferior temporal gyrus (BA 20/21/22). Furthermore, reading aloud activated a large network of regions in the left hemisphere including the angular gyrus (BA 19/22/37/39), frontal cortex (BA 6/8/9/10/46), subcentral area (BA 4/6/43), insula (BA 13), medial paracentral lobule (BA 31), and cingulate (BA 24/31). The engagement of middle-inferior frontal regions was observed also during letter presentation (BA

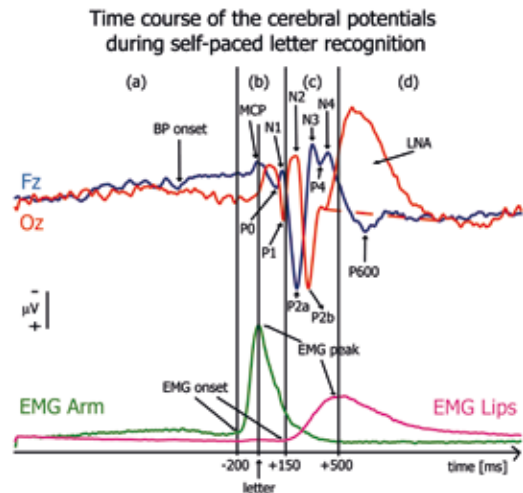


Fig. 4. – Schematic representation of the time course of the cerebral potentials recorded during self-paced letter recognition (i.e. *naming*): sample recordings from Fz (blue trace) and Oz (red trace) electrodes. Superimposition with the electromyographic activity of lips activated by overt articulation (purple trace) and of forearm muscles activated by button pressing (green trace) allows to subdivide the cerebral potentials into four main periods: (a) preparatory, (b) pre-lexical, (c) lexical, and (d) post-lexical period. BP = Bereitschaftspotential; MCP = Motor Cortex Potential; LNA = Late Negative Area (Chiarenza et al. 2004).



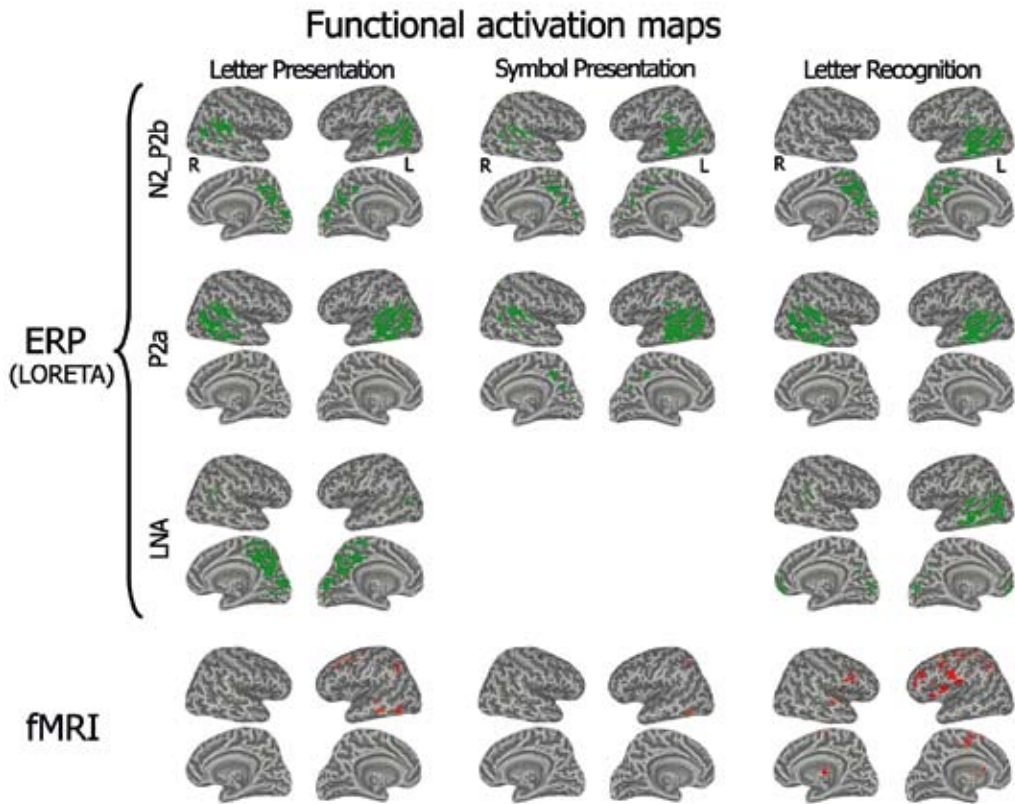


Fig. 5. – Superimposition of functional activations on inflated anatomical cortical surface: lateral and medial views of both hemispheres. LORETA maps (green) of the N2\_P2b, P2a, and LNA potentials and fMRI activation maps (red) are reported for the *letter presentation*, *symbol presentation*, and *letter recognition* tasks. R = right; L = left.

6/8/9) but was absent during symbol presentation. However, the left inferior parietal lobule (BA 40) and fusiform gyrus (BA 19/20/37) were similarly activated during letter and symbol presentation.

*ERPs-fMRI combination.* The superimposition of fMRI activation maps and LORETA current density maps showed a convergence of results in two specific brain regions (Table I): the left inferior temporal – middle occipital gyrus (BA 19/20/37) and the left middle-superior temporal gyrus (BA 21/22). The LORETA maps of the LNAf/LNAo components did not overlap with the corresponding fMRI maps. During letter and symbol presentation, clusters of inter-modality overlapping voxels were observed in the left fusiform gyrus for the N2\_P2b and P2a components, extending anteriorly to the inferior temporal gyrus (BA 20/21) for P2a during letter presentation. The superimposition of fMRI and LORETA maps during letter recognition was characterized by overlap in a small portion of the left supra-marginal gyrus (BA 40) for the N2\_P2b component, in the right middle temporal gyrus (BA 21/22) for the P2a component, and in the left angular gyrus for all the ERP components.

## DISCUSSION

The present work explored the neural correlates of single-letter reading by combining ERP and fMRI data separately recorded from healthy adults. Three different externally-paced reading tasks were applied within an event-related design: passive presentation of letters and of non-alphabetic symbols, and reading aloud of letters. Physiologically plausible and functionally independent components were extracted from averaged ERPs with ICA, and the spatial distribution of their neural sources was estimated with LORETA. Functional activation maps computed from fMRI data were superimposed to LORETA maps, thus highlighting the overlapping activations and the activated regions specifically revealed by each modality, in order to further understand the complementary contribution of the two methodologies to the study of early reading processes.

The results showed that ERP-fMRI integration was always confined on the lateral surface of the left hemisphere. This pattern of activation further supports the idea of a left-hemisphere dominance during linguistic tasks in right-handed subjects (86, 69). In particular, during letter presentation, the largest overlap between fMRI and LORETA maps was observed for the P2a potential in the inferior temporal-middle occipital gyrus (BA 19/20/37) and in the middle-superior temporal gyrus (BA 21/22). The P2a component is actually a robust potential (10-15  $\mu$ V) easily identifiable on averaged ERPs in all the frontal and central EEG channels. Therefore, the neural activation generating this potential likely drives the hemodynamic signal and dominates over that related to smaller waves. Overlap in the fusiform gyrus was also observed in correspondence to N2\_P2b, whose neural sources were located close to P2a sources. These results are compatible with previous studies that investigated the letter-sound correspondence with audiovisual presentation of single letters (88, 103), and further indicate that reading is a very complex phenomenon activating a large neuronal network including multimodal brain areas. This consideration also agrees with the bulk of previous studies in the literature reporting many different effects of manipulation of reading parameters and conditions both at the behavioural and physiological level (77, 85).

During symbol presentation, the fMRI-LORETA overlap was reduced and confined to the left fusiform gyrus, despite the potentials were morphologically similar to those recorded during letter presentation.

During letter recognition overlapping regions were specifically located in the left supramarginal gyrus (BA 40) in correspondence to N2\_P2b component, and in the left middle-superior temporal gyrus (BA 21/22) in correspondence to P2a component. Activation of the left middle-superior temporal gyrus and supramarginal gyrus has been associated to perception of one's own speech, and to the process of matching the actual auditory feedback with the internal representation of the feedback itself (92). Interestingly, LORETA results of the present experiment showed that these regions were engaged during all tasks, not only when explicit verbal-motor articulation was required. Therefore, their contribution appears to be equally important during covert reading, and may be possibly related to implicit phonological analysis. Furthermore, the observation of significant hemodynamic response of these regions during letter recognition only suggests that the contribution of these temporo-parietal networks is better represented by ERP recordings compared to functional imaging during silent reading.

Significantly different activations of the temporal cortex have been observed between normal and impaired readers during visual presentation of single characters (93, 98): in particular, the activation of the lateral temporo-parietal region was reduced in the left and increased in the right hemisphere in dyslexics as compared to controls. Furthermore, activity in the left posterior superior temporal sulcus has been associated to maturation of the phonological processing abilities in young readers (102). These studies suggest that the temporal cortex is crucially involved in phonological analysis of speech and the left angular gyrus likely plays a significant role in conversion of print to sound. In addition to functional abnormalities, significant structural modifications of the occipitotemporal cortex have been recently reported in dyslexic adolescents compared to controls (55). Therefore, since all these regions were fully engaged in this study, it might be feasible to apply this experimental design also for investigating pathological reading conditions.

In addition, this experiment provided further evidence of the functional differentiation between processing of letters and non-alphabetic symbols. Passive observation of symbols activated a reduced neuronal network, basically the left fusiform gyrus (BA 19/37) and the left inferior parietal lobule (BA 40), while letter presentation additionally engaged the left middle-inferior temporal (BA 21/22) and prefrontal regions (BA 6/9). The long-latency potentials LNaf and LNAo observed during letter presentation and recognition, respectively, could not be clearly identified during symbol presentation. Further differences were related to P2a sources, which were left-predominant on the lateral temporal and parietal regions, and extended medially in the cingulate and precuneus during symbol presentation, as compared to a symmetrical lateral distribution during letter presentation and recognition tasks. These results suggest that, despite their graphical similarity with symbols, letters activate a specific neuronal network with characteristic spatiotemporal dynamics of activation.

The significantly different patterns of activation observed during letter presentation and recognition suggest that explicit verbal-motor articulation engages functionally distinct brain processes in comparison with covert reading (12, 43, 78, 92). Despite the fMRI artifacts induced by facial movements, there is evidence that the neural substrates of silent and overt speech cannot be considered the same up the planning and execution of articulation movements, and therefore it is not fully correct to apply covert instead of overt speech paradigms just to reduce movement artifacts. In fact, an increased involvement of frontal regions was present during reading aloud, i.e. the left middle prefrontal cortex, left subcentral area (BA 4/6/43), right inferior frontal cortex (BA 6/9/44), and bilateral insula (BA 13). Previous fMRI studies have shown that the left insula has a crucial role in speech production, specifically in motor planning and programming, muscular coordination, phonological and sub-lexical spelling-to-sound processing (86, 38, 92, 13). Furthermore, the enhanced left-lateralization of N2\_P2b sources in the lateral temporo-occipital regions during letter recognition supports the hypothesis of early activation of reading-specific neuronal networks in the left hemisphere occurring when the subject has to explicitly read aloud.

Several reading-related brain regions were also significantly described. In particular, the left extrastriate cortex has been strongly related to single-letter identification (34, 29, 48, 83), the left fusiform gyrus and inferior frontal cortex to visual presentation of both objects and letters (23, 66, 67), and the left inferior parietal cortex (BA 40) and insula to letter recognition (51, 50, 68, 47). Significant engagement of the left precentral gyrus and premo-

tor cortex has been observed during visual perception, copying, and writing of letters, thus suggesting that writing motor processes are implicitly evoked during passive observation of letters (60, 47).

From a psychophysiological perspective, the approach applied in this study investigated the simplest unit of grapheme-phoneme association mechanisms, i.e. passive viewing and reading aloud of single letters. The use of isolated letters instead of words prevents any interference with semantic processes. Furthermore, this paradigm can be applied also to young children, without specific adaptations to account for their learning and cognitive development. Neuro-pathological studies have shown that the identification of letters is an early predictor of later reading success and distinguishes adult dyslexics (28, 84): the use of this pre-lexical skill is expected to be helpful to highlight the neurobiological and functional basis of reading in both healthy and impaired readers. It is important to observe that our experimental design was specifically developed for native Italian speakers: broadly applied word-rhyming tasks (8, 36, 101, 68, 44) are not appropriate since Italian is a highly transparent language, characterized by a perfect grapheme-phoneme matching.

The ERP components considered in the present work are comparable to a certain extent with previous studies of reading-related neurophysiological recordings. The potentials belonging to the *pre-lexical* period were not clearly distinguishable in the ICs: they are usually related to early visual perceptual processes and are characterized by small amplitude and marked inter-individual variability, that complicates their detection even on individual averaged ERPs (73, 26, 79). Considering the potentials of the *lexical* period, N2 corresponds to a posterior negativity occurring between 150–200 ms that has been reported by several ERP (“N2” – 108, 82; “N200” – 8, 35, 62, 65; “N170” – 64) and MEG studies (91, 97, 61). This potential has been related to automatic word form processing, to extraction of letter-shape information and to grapheme-phoneme association. In the literature, sources of N2-like components have been located in the inferior/ventral temporo-occipital cortex (108, 97, 61), similarly to the results described in this study. P2a was characterized by significantly higher amplitude on frontal and central regions and occurred earlier, usually around 200 ms, than P2b, that was dominant in the parietal and occipital regions and occurred later, around 300 ms. The differences in latency and scalp topography of these peaks suggest that they are likely generated by different brain sources: their distribution in two distinct ICs further supports this hypothesis, that is consistent with previous works of Dipole Source Modelling (46, 104) and with MEG and intracranial recordings studies (41, 40, 31). Magneto-encephalographic studies (90, 61) have suggested that P2a may represent “articulatory aspects of phonological processing and a motor preparation for oral output and actual vocalization” (90), while P2b could be related to phonological aspects of linguistic processing or attentional aspects of visual perception (72, 75, 19) or represent an interface between visual and linguistic domain (97). A recent ERP study (56) has identified two positive waves occurring at 170 and 250 ms respectively that resemble quite well the components P2a and P2b observed in our study. Lee and colleagues (56) have assigned to these potentials a possible role in early extraction of phonology during reading of Chinese pseudocharacters. Considering the *post-lexical* period (> 500 ms), the physiological meaning of LNAf and LNAo components is not precisely known and their marked inter-individual variability prevents their

reliable identification on individual averaged ERPs. However, these components could be probably related to higher order cognitive functions, that are usually elicited at long latencies and are characterized by highly variable potentials.

Stimuli duration was kept short so that letters were perceived as a *gestalt* and subjects' attention, cooperation and motivation were strongly recruited. Longer persistence would have likely reduced task difficulty and produced a facilitatory effect on brain activation (87). Moreover, short duration elicited foveal vision and limited eye saccadic movements, which are critical sources of artifacts for EEG recordings.

The statistical efficiency of localizing fMRI activations within ER-designs is better when ISI is properly jittered and randomized than when ISI is fixed and improves with the decreasing of mean ISI. Therefore, the transfer of conventional ERP recording protocols in the fMRI environment is perfectly feasible and do not necessarily sacrifice statistical power or efficiency of either technique (21). The application of a fairly short ISI in the present experiment allowed to successfully deal with the fMRI artifacts produced by articulation movements during reading aloud of letters, which could both mask and mimic BOLD responses. In fact, BOLD and movement-induced signal changes arise from different physical mechanisms, the former being sluggish and delayed, the latter being sharp and nearly instantaneous. Simulations and experiments on real data have demonstrated that ER-designs with varying ISI are the least susceptible to movement as compared to blocked designs and to fixed-ISI event-related designs (10).

Traditional and innovative strategies of signal processing were combined to analyze the electrical brain responses. ERPs are traditionally characterized by quantification of amplitude and latency of their positive and negative peaks. However, in contrast to the assumption that each peak represents the response of a functionally specific brain network, even if the actual source location is stable, peak latency may vary on the scalp due to the summation of activities of a number of brain areas with different time courses of activation (73). Therefore, it is not generally correct to assume a one-to-one correspondence between single potentials and discrete stages of information processing. PCA was first applied to averaged ERPs in order to reduce data dimensionality and successively ICA was used to estimate spatially overlapping and temporally independent brain sources that project on the cognitive potentials recorded on the scalp (4). The results showed that this procedure is easy to apply, is not affected by the subjective judgment of the experimenter and provides a synthetic and powerful description of cognitive ERPs.

Combination of different techniques implies that different signals are evaluated in the same reference space: since fMRI data are time series of volumetric images, EEG recordings should be converted into three-dimensional (3D) current density distribution maps modulated in time. Even if spatial resolution of neural sources estimated from ERPs was not optimal for the rather limited number of recording channels, the described procedure provided valuable results and can be applied when extended montages are available. In this experiment we had not robust *a priori* information to reliably constrain the source estimation process. The application of LORETA method for solving the EEG inverse problem allowed to estimate a distributed source configuration in the whole brain volume. This approach is physiologically plausible, since brain activation is usually distributed on the cortical surface rather than concentrated in a small patch of grey matter (105). Furthermore, EEG and fMRI

signals are actually generated by partly different phenomena and therefore convey similar but not exactly identical information: as a consequence, it is better to avoid mutual interference between EEG and fMRI signals to prevent from obtaining biased results.

This work has some limitations, mainly related to the limited number of subjects, that reduces statistical power and generalizability of results, and of EEG channels, that limits accuracy of localization of cerebral sources. Furthermore, ERP and fMRI data were recorded in two separate sessions, thus being not rigorously related to the “same” brain activity; on the other hand, separate acquisition offered the advantage of measuring clean signals, i.e. without any artifact related to mutual interference between EEG and fMRI equipments and undistorted by severe artifact filtering procedures.

## CONCLUSION

This work described an innovative procedure for combining neurophysiological and functional neuroimaging data. The grapheme-phoneme association mechanisms naturally active during reading were specifically investigated: despite some experimental limitations, the results support the validity of this approach, that correctly identifies the spatiotemporal dynamics of brain regions functionally involved in reading processes. The event-related protocol was effectively designed to avoid any possible bias deriving from separate acquisition of ERP and fMRI data.

The results showed the existence of letter-specific neuronal networks clearly differentiated from those involved during passive observation of non-alphabetic symbols. Furthermore, significantly different patterns of activation were found between passive observation and reading aloud of letters, that likely depend on functionally different processes beyond explicit verbal-motor articulation.

The results of the present experiment suggest that the role played by the inferior temporal-middle occipital gyrus is crucial and multifunctional for linguistic and reading processes: the reason may be related to the fact that it receives inputs from the visual system and strongly interacts with temporal auditory areas. Therefore, its spatial location and its strong interconnection with the main sensory systems may have favored its specialization in grapheme-phoneme matching.

This observation may be advanced as a working hypothesis for further investigating the role of left middle temporal-occipital lobe in reading and language, by possibly exploring the effects of voluntary intention to read, and the modulation of its activity in children and impaired readers.

*Acknowledgments.* – This research was partially supported by the Bioengineering Committee of the Milan Order of Engineers (Milan, Italy). The authors wish to thank Igor De Marchi and Barbara Sasselli for their support in signal recording at the Neuro-physio-pathology Laboratory, Az. Osp. “G. Salvini”, Rho Hospital (Rho, Milan, Italy) and Luigi Landini, professor at the Faculty of Engineering, University of Pisa (Pisa, Italy) for his support to images recording at the MRI Laboratory Fondazione “G. Monasterio”, CNR/Regione Toscana (Pisa, Italy) coordinated by Massimo Lombardi. We thank Lorenzo Sani and Daniela Bonino for comments and advices about the experimental paradigm and data analysis.

## REFERENCES

1. BABILONI, F., BABILONI, C., CARDUCCI, F., ROMANI, G.L., ROSSINI, P.M., BASILISCO, A., SALINARI, S., ASTOLFI, L. and CINCOTTI, F. Solving the neuroimaging puzzle: the multimodal integration of neuroelectromagnetic and functional magnetic resonance recordings. *Suppl Clin Neurophysiol*, **57**: 450-457, 2004a.
2. BABILONI, F., BABILONI, C., CARDUCCI, F., ROSSINI, P.M., BASILISCO, A., ASTOLFI, L. and CINCOTTI, F. Multimodal integration of EEG and functional magnetic resonance recordings. *Conf. Proc. IEEE Eng. Med. Biol. Soc.*, **7**: 5311-5314, 2004b.
3. BABILONI, F., MATTIA, D., BABILONI, C., ASTOLFI, L., SALINARI, S., BASILISCO, A., ROSSINI, P.M., MARCIANI, M.G. and CINCOTTI, F. Multimodal integration of EEG, MEG and fMRI data for the solution of the neuroimage puzzle. *Magn. Res. Imaging*, **22**(10): 1471-1476, 2004c.
4. BAILLET, S., MOSHER, J.C. and LEAHY, M. Electromagnetic brain mapping. *IEEE Signal Processing Magazine*, **18**(6): 14-30, 2001.
5. BANDETTINI, P.A. and UNGERLEIDER, L.G. From neuron to BOLD: new connections. *Nat. Neurosci.*, **4**(9): 864-866, 2001.
6. BELL, A.J. and SEJNOWSKI, T.J. An information-maximization approach to blind separation and blind deconvolution. *Neural Comput.*, **7**: 1129-1159, 1995.
7. BÉNDAR, C.-G., SCHÖN, D., GRIMAULT, S., NAZARIAN, B., BURLE, B., ROTH, M., BADIÉ, J.-M., MARQUIS, P., LIEGEOIS-CHAUVÉL, C. and ANTON, J.-L. Single-trial analysis of oddball event-related potentials in simultaneous EEG-fMRI. *Hum. Brain Mapp.*, **28**(7): 602-613, 2007.
8. BENTIN, S., MOUCHETANT-ROSTAING, Y., GIARD, M.H., ECHALLIER, J.F. and PERNIER, J. ERP manifestations of processing printed words at different psycholinguistic levels: time course and scalp distribution. *J. Cogn. Neurosci.*, **11**(3): 235-260, 1999.
9. BILLINGSLEY-MARSHALL, R.L., SIMOS, P.G. and PAPANICOLAOU, A.C. Reliability and validity of functional neuroimaging techniques for identifying language-critical areas in children and adults. *Dev. Neuropsychol.*, **26**(2): 541-563, 2004.
10. BIRN, R.M., COX, R.W. and BANDETTINI, P.A. Experimental designs and processing strategies for fMRI studies involving overt verbal responses. *Neuroimage*, **23**: 1046-1058, 2004.
11. BONMASSAR, G., SCHWARTZ, D.P., LIU, A.K., KWONG, K.K., DALE, A.M. and BELLIVEAU, J.W. Spatiotemporal brain imaging of visual-evoked activity using interleaved EEG and fMRI recordings. *Neuroimage*, **13**: 1035-1043, 2001.
12. BOOKHEIMER, S.Y., ZEFFIRO, T.A., BLAXTON, T., GAILLARD, W. and THEODORE, W. Regional cerebral blood flow during object naming and word reading. *Hum. Brain Mapp.*, **3**: 93-106, 1995.
13. BOROWSKY, R., CUMMINE, J., OWEN, W.J., FRIESEN, C.K., SHIH, F. and SARTY, G.E. FMRI of ventral and dorsal processing streams in basic reading processes: insular sensitivity to phonology. *Brain Topogr.*, **18**(4): 233-239, 2006.
14. CASAROTTO, S., BIANCHI, A.M., CERUTTI, S. and CHIARENZA, G.A. Principal Component Analysis for reduction of ocular artefacts in event-related potentials of normal and dyslexic children. *Clin. Neurophysiol.*, **115**(3): 609-619, 2004.
15. CHIARENZA, G.A. and CASAROTTO, S. Imparare a leggere: i meccanismi psicofisiologici. [Learning to read: the psychophysiological mechanisms]. *Quaderni ACP*, **11**(5): 212-215, 2004.
16. CHIARENZA, G.A., CASAROTTO, S. AND DE MARCHI, I. Chronology of reading processes. *Int. J. Psychophysiol.*, **65**(1-2): 85, 2004.
17. CHIARENZA, G.A., PAKOSTOPOULOS, D., GIORDANA, F. and GUARESCHI-CAZZULLO, A.

- Movement-related brain macropotentials during skilled performances. A developmental study. *Electroencephalogr. Clin. Neurophysiol.*, **56**: 373-383, 1983.
18. CHIARENZA, G.A., VILLA, M. and VASILE, G. Developmental aspects of Bereitschaftspotential in children during goal directed behavioural. *Int. J. Psychophysiol.*, **19**(2): 149-176, 1995.
  19. CORBETTA, M. Frontoparietal cortical networks for directing attention and the eye to visual locations: identical, independent, or overlapping neural systems? *Proc. Natl. Acad. Sci. USA*, **95**: 831-838, 1998.
  20. COX, R.W. AFNI©: software for analysis and visualization of functional magnetic resonance neuroimages. *Comput. Biomed. Res.*, **29**: 162-173, 1996.
  21. DALE, A.M. Optimal experimental design for event-related fMRI. *Hum. Brain Mapp.*, **8**: 109-114, 1999.
  22. DALE, A.M. and HALGREN, E. Spatiotemporal mapping of brain activity by integration of multiple imaging modalities. *Curr. Opin. Neurobiol.*, **11**: 202-208, 2001.
  23. DEHAENE, S., LE CLEC'H, G., POLINE, J.-B., LE BIHAN, D. and COHEN, L. The visual word form area: a prelexical representation of visual words in the fusiform gyrus. *Neuroreport* **13**(3): 321-325, 2002.
  24. DELORME, A. and MAKEIG, S. EEGLAB: an open source toolbox for analysis of single-trial EEG dynamics including independent component analysis. *J. Neurosci. Methods*, **134**: 9-21, 2004.
  25. DÉMONET, J.-F. The dynamics of language-related brain images. *Neurocase*, **11**: 148-150, 2005.
  26. DI RUSSO, F., MARTINEZ, A., SERENO, M.I., PITZALIS, S. and HILLYARD, S.A. Cortical sources of the early components of the visual evoked potential. *Hum. Brain Mapp.*, **15**(2): 95-111, 2002.
  27. DONCHIN, E. and HEFFLEY, E.F. Multivariate analysis of event related potential data: a tutorial review. Pp. 555-572. In: OTTO D. A. (Ed.), *Multidisciplinary perspectives in event-related brain potential research*. Washington, D.C., US Environmental Protection Agency, 1978.
  28. FLOWERS, D.L. Neuropsychological profiles of persistent reading disability and reading improvement. Pp. 61-77. In: LONG C. K., and JOSHI R. M. (Eds.), *Developmental and Acquired Dyslexia: Neuropsychological and Neurolinguistic Perspectives*, Boston, Kluwer, 1995.
  29. FLOWERS, D.L., JONES, K., NOBLE, K., VANMETER, J., ZEFFIRO, T.A., WOOD, F.B. and EDEN, G.F. Attention to single letters activates left extrastriate cortex. *Neuroimage*, **21**: 829-839, 2004.
  30. FOUCHER, J.R., OTZENBERGER, H. and GOUNOT, D. The BOLD response and the gamma oscillations respond differently than evoked potentials: an interleaved EEG-fMRI study. *BMC Neurosci.*, **4**: 22, 2003.
  31. GODEY, B., SCHWARTZ, D., DE GRAAF, J.B., CHAUVEL, P. and LIEGEOIS-CHAUVEL, C. Neuromagnetic source localization of auditory evoked fields and intracerebral evoked potentials: a comparison of data in the same patients. *Clin. Neurophysiol.*, **112**(10): 1850-1859, 2001.
  32. GOLDMAN, R.I., STERN, J.M., ENGEL, J. JR. and COHEN, M.S. Acquiring simultaneous EEG and functional MRI. *Clin. Neurophysiol.*, **111**: 1974-1980, 2000.
  33. GONZALEZ-ANDINO, S.L., PASCUAL-MARQUI, R.D., VALDÉS-SOSA, P.A., BISCAY-LIRIO, R., MACHADO, C., DIAZ, G., FIGUEREDO-RODRIGUEZ, P. and CASTRO-TORREZ, C. Brain electrical field measurements unaffected by linked earlobes reference. *Electroencephalogr. Clin. Neurophysiol.*, **75**: 155-160, 1990.
  34. GROS, H., BOULANOUAR, K., VILLARD, G., CASSOL, E. and CELSIS, P. Event-related functional magnetic resonance imaging study of the extrastriate cortex response to a categorically

- ambiguous stimulus primed by letters and familiar geometric figures. *J. Cereb. Blood Flow Metab.*, **21**: 1330-1341, 2001.
35. GROSSI, G. and COCH, D. Automatic word form processing in masked priming: an ERP study. *Psychophysiology*, **42**: 343-355, 2005.
  36. GROSSI, G., COCH, D., COFFEY-CORINA, S., HOLCOMB, P.J. and NEVILLE, H.J. Phonological processing in visual rhyming: a developmental ERP study. *J. Cogn. Neurosci.*, **13**(5): 610-625, 2001.
  37. GRÜNLING, C., LIGGES, M., HUONKER, R., KLINGERT, M., MENTZEL, H.-J., RZANNY, R., KAISER, W.A., WITTE, H. and BLANZ, B. Dyslexia: the possible benefit of multimodal integration of fMRI- and EEG-data. *J. Neural Transm.*, **111**: 951-969, 2004.
  38. GUENTHER, F. H. Neural control of speech movements. In: MEYER, A., and SCHILLER N. (Eds.), *Phonetics and phonology in language comprehension and production: differences and similarities*, Berlin, Mouton de Gruyter, 2003.
  39. HALCHENKO, Y.O., HANSON, S.J. and PEARLMUTTER, B.A. Multimodal integration: fMRI, MRI, EEG, MEG. Pp. 223-265. In: LANDINI, L., POSITANO, V., and SANTARELLI M.F. (Eds.), *Advanced Image Processing in Magnetic Resonance Imaging*, New York, Taylor and Francis CRC Press, 2005.
  40. HARI, R., HAMALAINEN, H., HAMALAINEN, M., KEKONI, J., SAMS, M. and TIHONEN, J. Separate finger representations at the human second somatosensory cortex. *Neuroscience*, **37**(1): 245-249, 1990.
  41. HARI, R., PELIZZONE, M., MAKELA, J.P., HALLSTROM, J., LEINONEN, L. and LOUNASMAA, O.V. Neuromagnetic responses of the human auditory cortex to on- and offsets of noise bursts. *Audiology*, **26**(1): 31-43, 1987.
  42. HORWITZ, B. and POEPEL, D. How can EEG/MEG and fMRI/PET data be combined? *Hum. Brain Mapp.*, **17**: 1-3, 2002.
  43. HUANG, J., CARR, T.H. and CAO, Y. Comparing cortical activations for silent and overt speech using event-related fMRI. *Hum. Brain Mapp.*, **15**: 39-53, 2001.
  44. HUANG, K., ITOH, K., SUWAZONO, S. and TSUTOMU, N. Electrophysiological correlates of grapheme-phoneme conversion. *Neurosci. Lett.*, **366**: 254-258, 2004.
  45. IANNETTI, G.D., NIAZY, R.K., WISE, R.G., JEZZARD, P., BROOKS, J.C.W., ZAMBREANU, L., VENNART, W., MATTHEWS, P.M. and TRACEY, I. Simultaneous recording of laser-evoked brain potentials and continuous, high-field functional magnetic resonance imaging in humans. *Neuroimage*, **28**(3): 708-719, 2005.
  46. JACOBSON, G.P. Magnetoencephalographic studies of auditory system function. *J. Clin. Neurophysiol.*, **11**(3): 343-364, 1994.
  47. JAMES, K.H. and GAUTHIER, I. Letter processing automatically recruits a sensory-motor brain network. *Neuropsychologia*, **44**: 2937-2949, 2006.
  48. JAMES, K. H., JAMES, T. W., JOBARD, G., WONG, A. C.-N. and GAUTHIER, I. Letter processing in the visual system: different activation patterns for single letters and strings. *Cogn., Affect. Behav. Neurosci.*, **5**(4): 452-466, 2005.
  49. JOBARD, G., CRIVELLO, F. and TZOURIO-MAZOYER, N. Evaluation of the dual route theory of reading: a metanalysis of 35 neuroimaging studies. *Neuroimage*, **20**: 693-712, 2003.
  50. JOSEPH, J.E., CERULLO, M.A., FARLEY, A.B., STEINMETZ, N.A. and MIER, C.R. fMRI correlates of cortical specialization and generalization for letter processing. *Neuroimage*, **32**: 806-820, 2006.
  51. JOSEPH, J.E., GATHERS, A.D. and PIPER, G.A. Shared and dissociated cortical regions for object and letter processing. *Brain Res. Cogn. Brain Res.*, **17**: 56-67, 2003.
  52. KOBAYASHI, T. and KURIKI, S. Principal Component Elimination Method for the improvement of S/N in evoked neuromagnetic field measurements. *IEEE Trans. Biomed. Eng.*, **46**(8): 951-958, 1999.

53. KOLES, Z.J. The quantitative extraction and topographic mapping of the abnormal components in the clinical EEG. *Electroencephalogr. Clin. Neurophysiol.*, **79**: 440-447, 1991.
54. KORNHUBER, H.H. and DEECKE, L. Hirnpotential-änderungen bei Willkürbewegungen und passiven Bewegungen des Menschen: Bereitschaftspotential und reafferente Potentiale. [Changes in the brain potential in voluntary movements and passive movements in man: readiness potential and reafferent potentials.] *Pflügers Archiv für die Gesamte Physiologie des Menschen und der Tiere*, **284**: 1-17, 1965.
55. KRONBICHLER, M., WIMMER, H., STAFFEN, W., HUTZLER, F., MAIR, A. and LADURNER, G. Developmental dyslexia: gray matter abnormalities in the occipitotemporal cortex. *Hum. Brain Mapp.*, **29**(5):613-625, 2008.
56. LEE, C.-Y., TSAI, J.-L., CHIU, Y.-C., TZENG, O.J. L. and HUNG, D.L. The early extraction of sublexical phonology in reading Chinese pseudocharacters: an event-related potentials study. *Language and Linguistics*, **7**(3): 619-636, 2006.
57. LEMIEUX, L., ALLEN, P.J., KRAKOW, K., SYMMS, M.R. and FISH, D.R. Methodological issues in EEG-correlated functional MRI experiments. *International Journal of Bioelectromagnetism*, **1**(1): 87-95, 1999.
58. LOGOTHETIS, N.K., PAULS, J., AUGATH, M., TRINATH, T. and OELTERMANN, A. Neurophysiological investigation of the basis of the fMRI signal. *Nature*, **412**: 150-157, 2001.
59. LOGOTHETIS, N.K. and WANDELL, B.A. Interpreting the BOLD signal. *Annu. Rev. Physiol.*, **66**: 735-769, 2004.
60. LONGCAMP, M., ANTON, J.-L., ROTH, M. and VELAY, J.-L. Visual presentation of single letters activates a premotor area involved in writing. *Neuroimage*, **19**: 1492-1500, 2003.
61. MARINKOVIĆ, K. Spatiotemporal dynamics of word processing in the human cortex. *The Neuroscientist*, **10**(2): 142-152, 2004.
62. MARTIN, C., NAZIR, T., THIERRY, G., PAULIGNAN, Y. and DÉMONET, J.-F. Perceptual and lexical effects in letter identification: an event-related potential study of the word superiority effect. *Brain Res.*, **1098**: 153-160, 2006.
63. MATHALON, D.H., WHITFIELD, S.L. and FORD, J.M. Anatomy of an error: ERP and fMRI. *Biol. Psychol.*, **64**: 119-141, 2003.
64. MAURER, U., BRANDEIS, D. and MCCANDLISS, B.D. Fast, visual specialization for reading in English revealed by the topography of the N170 ERP response. *Behav. Brain Funct.*, **1**(1): 13, 2005.
65. MAURER, U. and MCCANDLISS, B.D. The development of visual expertise for words: the contribution of electrophysiology. In: GRIGORENKO, E.L. and NAPLES A.J. (Eds.), *Single-Word Reading: Behavioral and biological perspectives*, Mahwah, NJ, Lawrence Erlbaum Associates, 2007.
66. MCCANDLISS, B.D., COHEN, L. and DEHAENE, S. The visual word form area: expertise for reading in the fusiform gyrus. *Trends Cogn. Sci.*, **7**(7): 293-299, 2003.
67. MCCANDLISS, B.D. and NOBLE, K.G. The development of reading impairment: a cognitive neuroscience model. *Ment. Retard. Dev. Disabil. Res. Rev.*, **9**(3): 196-204, 2003.
68. McDERMOTT, K.B., PETERSEN, S.E., WATSON, J.M. and OJEMANN, J.G. A procedure for identifying regions preferentially activated by attention to semantic and phonological relations using functional magnetic resonance imaging. *Neuropsychologia*, **41**: 293-303, 2003.
69. MECHELLI, A., CRINION, J.T., LONG, S., FRISTON, K.J., LAMBON RALPH, M.A., PATTERSON, K., MCCLELLAND, J.L. and PRICE, C.J. Dissociating reading processes on the basis of neuronal interactions. *J. Cogn. Neurosci.*, **17**(11): 1753-1765, 2005.
70. MENON, R.S., GATI, J.S., GOODYEAR, B.G., LUKNOWSKY, D.C. and THOMAS, C.G. Spatial and temporal resolution of functional magnetic resonance imaging. *Biochem. Cell Biol.*, **76**: 560-571, 1998.

71. MENON, V. and CROTTAZ-HERBETTE, S. Combined EEG and fMRI studies of human brain function. *Int. Rev. Neurobiol.*, **66**: 291-321, 2005.
72. MESULAM, M.M. A cortical network for directed attention and unilateral neglect. *Ann. Neurol.*, **10**(4): 309-325, 1981.
73. NÄÄTÄNEN, R. and PICTON, T. The N1 wave of the human electric and magnetic response to sound: a review and an analysis of the component structure. *Psychophysiology*, **24**(4): 375-425, 1987.
74. NOBLE, K.G. and MCCANDLISS, B.D. Reading development and impairment: behavioural, social, and neurobiological factors. *J. Dev. Behav. Pediatr.*, **26**: 370-378, 2005.
75. NOBRE, A.C., SEBESTYEN, G.N., GITELMAN, D.R., MESULAM, M.M., FRACKOWIAK, R.S. and FRITH, C.D. Functional localization of the system for visuospatial attention using positron emission tomography. *Brain*, **120**: 515-533, 1997.
76. NUNEZ, P. *Electric fields of the brain: the neurophysics of EEG*, New York: Oxford University Press, 1981.
77. PADOVANI, R., CALANDRA-BUONAURO, G., CACCIARI, C., BENUZZI, F., NICHELLI, P. Grammatical gender in the brain: evidence from an fMRI study on Italian. *Brain Res. Bull.*, **65**(4):301-308, 2005.
78. PALMER, E.D., ROSEN, H.J., OJEMANN, J.G., BUCKNER, R.L., KELLEY, W.M. and PETERSEN, S.E. An event-related fMRI study of overt and covert word stem completion. *Neuroimage*, **14**: 182-193, 2001.
79. PAMMER, K., HANSEN, P.C., KRINGELBACH, M.L., HOLLIDAY, I., BARNES, G., HILLEBRAND, A., SINGH, K.D. and CORNELISSEN, P.L. Visual word recognition: the first half second. *Neuroimage*, **22**: 1819-1825, 2004.
80. PAPAPOSTOPOULOS, D. Electrical activity of the brain associated with skilled performance. Pp.134-137. In: OTTO D.A. (Ed.), *Multidisciplinary perspectives in Event-related brain potential research*, Washington D.C., U.S. Environmental Protection Agency, Office of Research and Development, 1978.
81. PASCUAL-MARQUI, R.D., MICHEL, C.M. and LEHMANN, D. Low resolution electromagnetic tomography: a new method for localizing electrical activity in the brain. *Int. J. Psychophysiol.*, **18**: 49-65, 1994.
82. PERNET, C., BASAN, S., DOYON, B., CARDEBAT, D., DÉMONET, J.-F. and CELSIS, P. Neural timing of visual implicit categorization. *Brain Res. Cogn. Brain Res.* **17**: 327-338, 2003.
83. PERNET, C., CELSIS, P. and DÉMONET, J.-F. Selective response to letter categorization within the left fusiform gyrus. *Neuroimage*, **28**: 738-744, 2005.
84. PERNET, C., VALDOIS, S., CELSIS, P. and DÉMONET, J.-F. Lateral masking, levels of processing and stimulus category: A comparative study between normal and dyslexic readers. *Neuropsychologia*, **44**: 2374-2385, 2006.
85. PERU, A., FACCIOLI, C., TASSINARI, G. Stroop effects from 3 to 10 years: the critical role of reading acquisition. *Arch. Ital. Biol.*, **144**: 45-62, 2006.
86. PRICE, C.J. The anatomy of language: contributions from functional neuroimaging. *J. Anat.*, **197**: 335-359, 2000.
87. PRICE, C.J., WISE, R.J., WATSON, J.D., PATTERSON, K., HOWARD, D. and FRACKOWIAK, R.S. Brain activity during reading. The effects of exposure duration and task. *Brain*, **117**: 1255-1269, 1994.
88. RAI, T., UUTELA, K. and HARI, R. Audiovisual integration of letters in the human brain. *Neuron*, **28**: 617-625, 2000.
89. SAAD, Z.S., CHEN, G., REYNOLDS, R.C., CHRISTIDIS, P.P., HAMMET, K.R., BELLGOWAN, P.S.F. and COX, R.W. Functional imaging analysis contest (FIAC) analysis according to AFNI and SUMA. *Hum. Brain Mapp.*, **27**(5): 417-424, 2006.

90. SALMELIN, R., HELENIUS, P. and SERVICE, E. Neurophysiology of fluent and impaired reading: a magnetoencephalographic approach. *J. Clin. Neurophysiol.*, **17**: 163-174, 2000.
91. SALMELIN, R., SERVICE, E., KIESILÄ, P., UUTELA, K. and SALONEN, O. Impaired visual word processing in dyslexia revealed with magnetoencephalography. *Ann. Neurol.*, **40**: 157-162, 1996.
92. SHUSTER, L.I. and LEMIEUX, S.K. An fMRI investigation of covertly and overtly produced mono- and multisyllabic words. *Brain Lang.*, **93**: 20-31, 2005.
93. SIMOS, P.G., BREIER, J.I., FLETCHER, J.M., BERGMAN, E. and PAPANICOLAOU, A.C. Cerebral mechanisms involved in word reading in dyslexic children: a magnetic source imaging approach. *Cereb. Cortex*, **10**: 809-816, 2000.
94. SINGH, M., KIM, S. and KIM, T.-S. Correlation between BOLD-fMRI and EEG signal changes in response to visual stimulus frequency in humans. *Magn. Res. Med.*, **49**: 108-114, 2003.
95. STERN, E. and SILBERSWEIG, D.A. Advances in functional neuroimaging methodology for the study of brain systems underlying human neuropsychological function and dysfunction. *J. Clin. Exp. Neuropsychol.*, **23**(1): 3-18, 2001.
96. TALAIRACH, J. and TOURNOUX, P. *Co-planar stereotaxic atlas of the human brain*, New York: Thieme Medical Publishers, 1988.
97. TARKIAINEN, A., HELENIUS, P., HANSEN, P.C., CORNELISSEN, P.L. and SALMELIN, R. Dynamics of letter string perception in the human occipitotemporal cortex. *Brain*, **122**: 2119-2131, 1999.
98. TEMPLE, E., POLDRACK, R.A., SALIDIS, J., DEUTSCH, G.K., TALLAL, P., MERZENICH, M.M. and GABRIELI, J.D. Disrupted neural responses to phonological and orthographic processing in dyslexic children: an fMRI study. *Neuroreport*, **12**(2): 299-307, 2001.
99. TOWLE, V.L., BOLANOS, J., SUAREZ, D., TAN, K., GRZESZCZUK, R., LEVIN, D.N., CAKMUR, R., FRANK, S.A. and SPIRE, J.P. The spatial location of EEG electrodes: Locating the best-fitting sphere relative to cortical anatomy. *Electroenceph. Clin. Neurophysiol.*, **86**: 1-6, 1993.
100. TSAI, A.C., LUOI, M., JUNG, T.-P., ONTON, J.A., CHENG, P.E., HUANG, C.-C., DUANN, J.-R. and MAKEIG, S. Mapping single-trial EEG records on the cortical surface through a spatiotemporal modality. *Neuroimage*, **32**: 195-207, 2006.
101. TURKELTAUB, P.E., EDEN, G.F., JONES, K.M. and ZEFFIRO, T.A. Meta-analysis of the functional neuroanatomy of single-word reading: method and validation. *Neuroimage*, **16**: 765-780, 2002.
102. TURKELTAUB, P.E., GAREAU, L., FLOWERS, D.L., ZEFFIRO, T.A. and EDEN, G.F. Development of neural mechanisms for reading. *Nat. Neurosci.*, **6**: 767-773, 2003.
103. VAN ATTEVELDT, N., FORMISANO, E., GOEBEL, R. and BLOMERT, L. Integration of letters and speech sounds in the human brain. *Neuron*, **43**: 271-282, 2004.
104. VERKINDT, C., BERTRAND, O., THEVENET, M. and PERNIER, J. Two auditory components in the 130-230 ms range disclosed by their stimulus frequency dependence. *Neuroreport*, **5**(10): 1189-1192, 1994.
105. VITACCO, D., BRANDEIS, D., PASCUAL-MARQUI, R.D. and MARTIN, E. Correspondence of event-related potential tomography and functional magnetic resonance imaging during language processing. *Hum. Brain Mapp.*, **17**: 4-12, 2002.
106. WARD, B.D. Simultaneous inference for fMRI data. [On-line] Available: <http://afni.nimh.nih.gov/pub/dist/doc/manual/AlphaSim.pdf>, 2000.
107. WARD, B.D. Deconvolution analysis of fMRI time series data. [On-line] Available: <http://afni.nimh.nih.gov/pub/dist/doc/manual/Deconvolvem.pdf>, 2006.
108. WIJERS, A.A., LANGE, J.J., MULDER, G. and MULDER, L.J.M. An ERP study of visual spatial attention and letter target detection for isoluminant and nonisoluminant stimuli. *Psychophysiology*, **34**: 553-565, 1997.

## APPENDIX A

Estimation of neural sources requires first to solve the associated *forward problem*, i.e. mapping a known configuration of brain sources to an array of EEG sensors. Supposing neural sources are distributed on a 3D lattice covering the whole brain, scalp measurements are related to electrical generators as follows:

$$\Phi = \mathbf{K} \cdot \mathbf{J} + \mathbf{n}$$

$(M,1) \quad (M,3P) \quad (3P,1) \quad (M,1)$

where  $\Phi$  is the vector of  $M$  instantaneous scalp recordings,  $\mathbf{K}$  is the *lead field* matrix,  $\mathbf{J}$  is the vector of strength of  $P$  current dipoles (three components each, along  $x,y,z$  Cartesian axes) distributed in the lattice and  $\mathbf{n}$  is a noise vector. The generic  $r$ -th row of matrix  $\mathbf{K}$  is:

$$\mathbf{K}_{r,:} = [k_{r,1}(x) \quad k_{r,1}(y) \quad k_{r,1}(z) \quad \cdots \quad k_{r,p}(x) \quad k_{r,p}(y) \quad k_{r,p}(z) \quad \cdots \quad k_{r,p}(x) \quad k_{r,p}(y) \quad k_{r,p}(z)]$$

with

$\{k_{r,p}(x) \quad k_{r,p}(y) \quad k_{r,p}(z)\}$  being the electrical activity due to the  $x,y,z$  components of the  $p$ -th dipole at the  $r$ -th sensor.

Since  $\Phi$  is known and  $\mathbf{K}$  is obtained from solving the forward problem, current density distribution  $\mathbf{J}$  can be estimated as:

$$\hat{\mathbf{J}} = \mathbf{T} \cdot \Phi$$

$(3P,1) \quad (3P,M) \quad (M,1)$

with  $\mathbf{T}$  being a generalized inverse of  $\mathbf{K}$ :

$$\mathbf{T} = \mathbf{W}^{-1} \mathbf{K}' [\mathbf{K} \mathbf{W}^{-1} \mathbf{K}']^+$$

with apex ' indicating transpose and  $[\bullet]^+$  indicating the Moore-Penrose pseudoinverse matrix. Solution of the *inverse problem* by maximizing smoothness can be expressed as follows:

$$\min_{\mathbf{J}} \|\mathbf{J}' \cdot \mathbf{W} \cdot \mathbf{J}\|^2 \quad \text{under constraint } \Phi = \mathbf{K} \mathbf{J}$$

where:

$$\mathbf{W} = (\Omega \otimes \mathbf{I}_3) \cdot \mathbf{B}' \cdot \mathbf{B} \cdot (\Omega \otimes \mathbf{I}_3)$$

$(3P,3P)$

with  $\otimes$  denoting the **Kronecker product**,  $\mathbf{I}_N$  being an  $(N,N)$  identity matrix,  $\Omega$  a square diagonal matrix computed as:

$$\Omega_{(P,P)} = [\Omega_{h,h}] = \sqrt{\sum_{j=1}^M \mathbf{K}'_{j,h} \mathbf{K}_{j,h}}$$

and  $\mathbf{B}$  implementing a discrete Laplacian operator:

$$\left\{ \begin{array}{l} \mathbf{B} = \frac{6}{d^2} (\mathbf{A} - \mathbf{I}_{3P}) \text{ with: } \mathbf{A} = \mathbf{A}_0 \otimes \mathbf{I}_3, \mathbf{A}_0 = \frac{1}{2} (\mathbf{I}_M + [\text{diag}(\mathbf{A}_1 \mathbf{1}_M)]^{-1}) \mathbf{A}_1 \\ [\mathbf{A}_1]_{\alpha\beta} = \begin{cases} (1/6), & \text{if } \|\mathbf{v}_\alpha - \mathbf{v}_\beta\| = d \\ 0, & \text{otherwise} \end{cases}, \forall \alpha, \beta = 1 \dots P \end{array} \right\}$$

where  $\text{diag}(\mathbf{A}_1 \mathbf{1}_p)$  denotes a diagonal matrix with diagonal elements defined by the elements of the  $(M,1)$  matrix  $\mathbf{A}_1 \mathbf{1}_p$  with  $\mathbf{1}_p$  being a  $(P,1)$  matrix comprised of ones and  $\mathbf{v}_p$  is the Cartesian position vector of the  $p$ -th source in the brain volume.  $\mathbf{B}^{-1}$  is actually a discrete spatial smoothing operator and therefore the estimated solution is the smoothest one.

